

7N-02  
197245  
338

# TECHNICAL NOTE

## D-184

AN EXPERIMENTAL INVESTIGATION AT A MACH NUMBER OF 4.95 OF  
FLOW IN THE VICINITY OF A  $90^\circ$  INTERIOR CORNER  
ALINED WITH THE FREE-STREAM VELOCITY

By P. Calvin Stainback

Langley Research Center  
Langley Field, Va.

NATIONAL AERONAUTICS AND SPACE ADMINISTRATION  
WASHINGTON

February 1960

(NASA-TN-D-184) AN EXPERIMENTAL  
INVESTIGATION AT A MACH NUMBER OF 4.95 OF  
FLOW IN THE VICINITY OF A  $90^\circ$  INTERIOR  
CORNER ALINED WITH THE FREE-STREAM VELOCITY  
(NASA) 33 p

N89-70580

Unclas  
00/02 0197245

## NATIONAL AERONAUTICS AND SPACE ADMINISTRATION

## TECHNICAL NOTE D-184

AN EXPERIMENTAL INVESTIGATION AT A MACH NUMBER OF 4.95 OF  
FLOW IN THE VICINITY OF A 90° INTERIOR CORNER  
ALINED WITH THE FREE-STREAM VELOCITY

By P. Calvin Stainback

## SUMMARY

An experimental investigation was made to determine the effects of the shock—boundary-layer interaction on the static pressure and heat-transfer rate in the vicinity of an interior corner formed by the normal intersection of two planes where the line of intersection was alined with the free-stream velocity. The investigation was made at a nominal Mach number of 4.95 and a stagnation temperature of 400° F. The nominal Reynolds number for the heat-transfer investigation ranged from  $1.95 \times 10^6$  to  $74.17 \times 10^6$  per foot and for the pressure test, from  $15.19 \times 10^6$  to  $74.17 \times 10^6$  per foot.

The results of the investigation indicated that the static pressure in the vicinity of the corner was from 10 to 12 percent greater than the pressure on a flat plate for the same free-stream conditions. The heat-transfer investigation indicated that the laminar-flow heat-transfer rate in the vicinity of the corner was higher than theoretical values for a flat plate at the same test conditions. For a Reynolds number of  $3.39 \times 10^6$  per foot, the increase was about 50 percent for stations 0.10 inch from the corner. The effect of the corner on the heat-transfer rate decreased with both distance from the corner and increasing unit Reynolds number. The effect of the corner on the turbulent-flow heat-transfer rate and the transition Reynolds number was negligible.

## INTRODUCTION

The phenomenon of shock—boundary-layer interaction has become of increasing importance in aerodynamics as attempts have been made to propel aircrafts and missiles to higher and higher speeds. It has been found that at high speeds the shock—boundary-layer interaction on simple shapes (flat plates, wedges, and cones) can appreciably alter the aerodynamic characteristics of these shapes (ref. 1). The question arises as to what extent will shock—boundary-layer interaction alter the

aerodynamic characteristics of more complex shapes of possible importance in aerodynamics. For example, what effect will shock—boundary-layer interaction have on the flow in the vicinity of an interior corner formed by the normal intersection of two planes where flow is directed parallel to the line of intersection (hereafter noted the corner-flow problem)? It is expected that some interaction between the normally undisturbed flat-plate boundary layer will occur in the vicinity of an interior corner when the radius of the corner is of the order of the boundary-layer thickness. This interaction can, for high-speed compressible flow, affect the flow external to the boundary layer as a result of induced shocks. Therefore, the boundary layer in the vicinity of the corner will be influenced by the mutual interference between normally undisturbed flat-plate boundary layers and by the mutual interaction between the boundary layer and the external flow.

There appears to be no compressible-flow solution for the corner-flow problem. There are, however, solutions to the problem for an incompressible fluid. With the assumption of incompressible flow, the only phenomenon present is the mutual interference between the otherwise undisturbed flat-plate boundary layers in the vicinity of the corner.

The first attempt to solve the incompressible corner-flow problem was apparently made by Loiziansky (ref. 2) and by Loitsianskii and Bolshakov (ref. 3). In their analysis a solution to the problem was obtained by the Kármán-Pohlhausen integral method. Carrier (ref. 4) obtained a solution to the problem by solving the boundary-layer equations in three dimensions. Sowerby and Cooke (ref. 5) solved the problem by using a modified form of the Rayleigh method.

The results obtained in references 3 to 5 indicated that the mutual interference between the laminar boundary layers in the vicinity of a corner resulted in a reduced drag as compared with the drag on an isolated flat plate. This reduction in drag for a 90° interior corner ranged from 12 percent (ref. 3) to 30 percent (ref. 5) when the width of the planes forming the corner was of the order of the interaction width. The interaction width was given as follows:

$$\frac{y}{x} = \frac{c}{\sqrt{N_{Re,x}}} \quad (1)$$

where  $c$  is a constant ranging in value from 5 (ref. 4) to 8.3 (ref. 3),  $y$  is distance from the corner,  $x$  is distance from leading edge, and  $N_{Re,x}$  is free-stream Reynolds number based on distance from leading edge.

The reduction in drag predicted by these theories would indicate a reduction in heat transfer in the vicinity of the corner if a form of

Reynolds analogy is assumed. However, the results obtained by assuming incompressible flow probably require modification before they can be applied to flow conditions where compressibility effects are present; and for supersonic flow, the results are of questionable value as a result of shock—boundary-layer interaction. The effect of the corner on boundary-layer transition is another problem to be considered.

The corner-flow problem is of interest for high-speed compressible flow since many present-day flight configurations have components which can be approximated by  $90^\circ$  interior corner. It is the purpose of the present paper to present pressure and heat-transfer measurements made on a  $90^\circ$  corner formed by the intersection of two flat plates where the line of intersection is aligned with the free-stream velocity. The nominal test-section Mach number and stagnation temperature for the investigation were 4.95 and  $400^\circ$  F, respectively. The nominal Reynolds number for the heat-transfer test ranged from  $1.95 \times 10^6$  to  $74.17 \times 10^6$  per foot and for the pressure test, from  $15.19 \times 10^6$  to  $74.17 \times 10^6$  per foot.

#### SYMBOLS

$c_m$	specific heat of model material
$c_{p,\infty}$	free-stream specific heat of a gas at constant pressure
$N_{Re}$	unit Reynolds number based on free-stream conditions
$N_{Re,x}$	Reynolds number based on free-stream conditions and distance from the leading edge
$N_{St}$	Stanton number based on free-stream conditions
$p$	model static pressure
$p_t$	free-stream stagnation pressure
$p_\infty$	free-stream static pressure
$q_{aero}$	aerodynamic heat-transfer rate
$q_{cond}$	conduction heat-transfer rate
$q_{stor}$	heat-storage rate

$T_m$	model material temperature	.
$T_r$	recovery temperature	.
$T_t$	stagnation temperature	
$T_w$	model wall temperature	
$T_\infty$	free-stream static temperature	
$t$	time	
$U_\infty$	free-stream velocity	L 5 2 1
$X, Y, Z$	coordinate axes, X-axis parallel to, and Y- and Z-axes transverse to, the free-stream direction	
$x, y, z$	distances along corresponding coordinate axes	
$\eta_r$	recovery factor	.
$\rho$	gas density	.
$\rho_m$	density of model material	
$\rho_\infty$	free-stream density	
$\tau$	model skin thickness	
Subscripts:		
$a$	apparent heat-transfer rate	
$c$	corner model	
$e$	quantities associated with the excess mass in corner of heat-transfer model	.
$fp$	flat-plate model	

## DESCRIPTION OF MODELS

The corner models were formed from two 0.50-inch-thick flat plates intersecting to form a  $90^\circ$  interior corner, 4 inches by 4 inches in the transverse direction and 10 inches long (fig. 1). The model was tested with the line of intersection aligned with the free-stream velocity.

### Pressure Model

The corner pressure model was fabricated from two flat plates which were machined from 0.50-inch-thick stainless-steel bar stock. The corner was formed by assembling the plates perpendicular to each other. Leading edges of the flat plates were machined to knife edges by beveling the plates  $20^\circ$ . The leading-edge thickness was  $0.0010 \pm 0.0005$  inch. General model dimensions are shown in figure 2.

Because of the expected symmetry of flow, only one interior face of the model was instrumented. A total of 28 static-pressure orifices were located on this face. The orifices were located to provide the greatest number of pressure readings in the vicinity of the corner and the leading edge. The coordinates of the pressure orifices are given in table I.

The model was tested as a flat plate by removing one plate forming the corner. A narrow plate was added to the instrumented side to eliminate any end effects on the measured pressures (fig. 2). As a result of testing the model both as a flat plate and as a corner model, the data could be reduced to a form which would eliminate, insofar as possible, any tunnel effects.

### Heat-Transfer Models

The corner heat-transfer model was machined from a single piece of 17-4PH stainless-steel bar stock. The plates which formed the corner were 0.50 inch thick, and the instrumented side was counterbored from its exterior face to form the thermocouple stations (fig. 2). The diameter of the cavity was 0.50 inch. The depth of the counterboring operation was controlled to produce a model skin thickness of 0.030 inch over the entire diameter of the cavity. In the vicinity of the leading edge, the diameter of the counterbored holes was reduced to 0.030 inch because of space limitations. In the vicinity of the corner, adjacent holes overlapped; when this occurred, a slot was machined to accommodate the thermocouples. All the cavities were shielded from the test-section flow by the mounting strut or by cover plates.

At the corner two counterbore operations,  $90^\circ$  apart, were made per station in order to form a corner with a 0.030-inch-thick wall (fig. 2). As a result of this method of machining, an excess mass 0.030- by 0.030-inch existed opposite the line of intersection of the planes forming the corner. This excess mass received no direct aerodynamic heating from the model surface; the heat stored in this mass was received from adjacent metal by conduction. Thermocouples were located on the corner of this excess mass diagonally opposite the interior corner exposed to the air stream. These thermocouples were used to estimate the conduction effect of the excess mass in the corner on the thermocouples located 0.10 inch from the corner.

A total of forty-one 0.010-inch-diameter iron-constantan thermocouples were installed in the model. The thermocouple junctions were made by spot-welding individual thermocouple wires to the reverse side of the model skin as shown in figure 2. The thermocouples were located to give the greatest number of temperature readings in the vicinity of the corner and the leading edge. The coordinates of the thermocouple stations are given in table II. At three stations, three thermocouples were installed in the same cavity to provide measurements required to estimate the conduction effects of the thick model wall on the thermocouple measurements at the center of the instrumented skin (fig. 2).

The corner was formed with the minimum radius of curvature possible, and the radius was measured to be approximately 0.006 inch. The leading edge of the model was measured and found to be less than 0.0005 inch. The surface finish of the model was uniform and ranged from 7 to 10 microinches.

A temperature-sensitive paint<sup>1</sup> investigation was conducted to gain further insight into the heat-transfer rate in the vicinity of the corner. In order to conduct this investigation, a third model was constructed. This model was fabricated from wood to provide a material which would reduce the effect of lateral conduction on the results.

## TEST PROCEDURE

Testing of the corner model was conducted at the Langley gas dynamics laboratory in a 9-inch axially symmetric blowdown jet at a nominal Mach number and stagnation temperature of 4.95 and  $400^\circ$  F, respectively. The test-section Reynolds number for the heat-transfer test ranged from  $1.95 \times 10^6$  to  $74.17 \times 10^6$  per foot and for the pressure investigation, from

---

<sup>1</sup>The temperature-sensitive paint, which carried the trade name "Thermocolor" (presently sold under the label "DetectoTemp"), was procured from the Curtiss-Wright Corporation, Princeton Division.

15.19  $\times 10^6$  to 74.17  $\times 10^6$  per foot. The jet exhausted to the atmosphere for all Reynolds numbers greater than 12.24  $\times 10^6$  per foot. For Reynolds numbers less than 12.24  $\times 10^6$  per foot, the jet exhausted to the laboratory vacuum system.

L  
5  
2  
1  
When the jet was exhausted to the vacuum system, the main air valve to the settling chamber was adjusted to prevent full opening of the valve. This method of testing was necessary to reduce the starting time of the jet because of valve opening time. The possible influence of the partly opened valve on test-section conditions was investigated by placing a stagnation pressure probe in the test section at a location which corresponded to the midchord of the model instrumented surface. Data were obtained with the probe over the range of conditions run during the corner investigation. The test section Mach number variation with stagnation pressure was computed from these data, and the results are presented in figure 3. The figure indicates that the partly opened main air valve had no apparent effect on test-section static conditions. The Mach number variation with stagnation pressure, shown in figure 3, was used throughout the investigation to calculate free-stream conditions.

Pressure tests were conducted with the model mounted in the test section prior to starting the jet. The pressures were indicated on a 120-inch butyl phthalate manometer board. The manometer board sump was evacuated to approximately test-section static pressure by a vacuum pump to reduce running time. The sump pressure was indicated on a single-leg mercury manometer which was vented to the atmosphere.

For the heat-transfer investigation, the jet was brought up to the desired operating conditions with the model outside the test section. After steady operation had been obtained, a vertical door in the test section was retracted; and the isothermal model, which was strut mounted (see fig. 2) on a second door that was actuated by a horizontal pneumatic cylinder, was inserted into the test section. The transient heating time, between the instant when the model initially entered the test-section door and the instant when the model was in its proper position in the test section, was less than 0.05 second. The model was removed from the test section after about 4 seconds and was brought to isothermal conditions, approximately room temperature, by suitable cooling. A more complete description of the jet and this method of testing can be found in reference 6.

The wooden model fabricated for the temperature-sensitive paint investigation was tested in a manner similar to that for the heat-transfer model.

## REDUCTION OF DATA

## Pressure Data

The pressure data were reduced to two forms: (1) the increase in the pressure on the model over the tunnel free-stream static pressure was divided by the tunnel static pressure and (2) the increase in the static pressure on the corner model over the flat-plate model was divided by the flat-plate static pressure.

## Heat-Transfer Data

Heat-transfer data were obtained by recording the temperature-time history of the model on a multichannel oscillograph. The heat-transfer rate to the model was calculated with the use of the following equation:

$$q_{\text{stor}} = \rho_m c_m \tau \frac{\partial T_m}{\partial t} \quad (2)$$

The heat-storage rate (also noted as the apparent aerodynamic heating rate) expressed in equation (2) can be equated to the aerodynamic heating rate, if it is assumed that the heat transferred to the model by aerodynamic effects is essentially stored in the model in the vicinity of the thermocouple (lateral conduction negligible) and is correctly indicated by the temperature measured on the reverse side of the skin (normal conduction infinite). The equation also assumes that the effect of radiation is negligible; this is true as a result of the low absolute temperatures involved throughout the test. The effect of lateral heat conduction on the apparent heat-transfer rates was investigated theoretically by using the results of reference 7. The unsteady-flow heat-conduction problem solved in reference 7 applies only to wires and semi-infinite slabs (one dimensional); therefore, the results can only be used to estimate the lateral conduction effects for the model stations that were milled slots. The correction to the apparent heating rate for stations located in the milled slots (0.50 inch wide) was essentially zero if the data were reduced for a time after the initial temperature rise of 0.25 second. For stations in the 0.30-inch-wide slots, the lateral conduction effects resulted in apparent heating rates which, for the highest rates, were about 2 percent lower than the actual heating rate. This error would be less for heating rates lower than the maximum.

The theory of reference 7 assumed a constant-temperature heat sink at the ends of the test specimen; and as a result of this assumption, the theory is unsuited for evaluating the effect of the 0.030- by 0.030-inch excess mass in the corner on the thermocouples located 0.10 inch from the corner, inasmuch as the temperature of this mass increased significantly during a test. An approximate method was developed to

estimate the error caused by the excess mass by using the measured temperature-time history of the excess mass. This method for estimating the conduction effect is outlined in the appendix. The approximation indicated that the apparent heating rate, calculated from the data obtained from the thermocouples located 0.10 inch from the corner, was less than 7.5 percent below the actual aerodynamic heating rate.

Unpublished theoretical calculations have been made by the Langley gas dynamics laboratory to estimate the effects of conduction in a cylindrical disk which is heated at a rate that is a function of its temperature and bounded by a constant-temperature heat sink. These results indicated that the difference between the actual and apparent aerodynamic heating rates was essentially zero for stations located in the center of a 0.50-inch-diameter cavity, if the data were reduced for a time after the initial temperature rise of 0.25 second. For the 0.30-inch-diameter cavity the error could be as much as 9 percent for the maximum heating rate experienced.

The data obtained from the multi-instrumented cavities indicated that the conduction effect resulted in an error of less than 10 percent between the apparent and actual aerodynamic heating rate for stations located in the 0.50-inch cavities. The difference between the heat-transfer rate computed from data obtained with the thermocouple located in the center of the 0.50-inch cavity and those located nearer the wall in the same cavity was about 10 percent. This result indicated that the measurements made in the 0.30-inch-diameter cavity were probably in error no more than 10 percent.

The effect of finite normal conduction on the apparent heat-transfer rate, resulting from attaching the thermocouples to the reverse side of the model skin, was investigated theoretically by the results of reference 8. The theoretical calculations indicated that finite normal conduction resulted in an indicated heating rate which was in error less than 2 percent for the highest heating rates experienced, if the data were reduced for a time after the initial temperature rise of 0.25 second.

Since the conduction and radiation errors were found to be small, equation (2) was used to calculate the aerodynamic heat-transfer rate to the model without the inclusion of the estimated corrections. The aerodynamic heat-transfer rate can be expressed as

$$q_{\text{aero}} = N_{\text{St}} U_{\infty} \rho_{\infty} c_{p,\infty} (T_r - T_w) \quad (3)$$

and with the use of equation (2), the following expression for the Stanton number can be obtained:

$$N_{St} = \frac{\rho_m c_m \tau \frac{\partial T_m}{\partial t}}{U_\infty \rho_\infty c_{p,\infty} (T_r - T_w)} \quad (4)$$

The change in temperature with respect to time  $\frac{\partial T_m}{\partial t}$  used in equation (4) was obtained by measuring the slope of the temperature-time curve at 0.25 second after the initial temperature rise. The slopes were read on an optical comparator and are estimated to be correct within  $\pm 0.5^\circ$ . The model wall temperature was calculated from data taken from the oscillograph trace at the point where the slope was measured. At 0.25 second after the initial temperature rise, the model was still essentially isothermal since the maximum increase in the temperature was about  $40^\circ$  F. The manufacturer's recommended value was used for the model material density. An empirical relationship was obtained from reference 9 for the specific-heat variation of the model material with temperature. The model skin thickness for each station was measured when the model was constructed.

The recovery temperature is given by

$$T_r = \eta_r (T_t - T_\infty) + T_\infty \quad (5)$$

The recovery factor  $\eta_r$  for laminar and turbulent flow was obtained from the square root and cube root of the free-stream Prandtl number, respectively. In the transition region, the turbulent-flow recovery factor was used.

The test-section velocity, density, and static temperature were obtained from the estimated test-section Mach number (fig. 3) and the measured stagnation conditions. The free-stream specific heat  $c_{p,\infty}$  was used throughout the calculations and was estimated from reference 10 from the mean conditions for the tests.

## DISCUSSION OF RESULTS

### Pressure Data

Representative plots of the static-pressure data for both the flat-plate and corner models are presented in figures 4 and 5. In figure 4, the pressure ratio  $(p - p_\infty)/p_\infty$  for both the flat plate and the corner model is plotted against distance along the model for several values of

y and several unit Reynolds numbers. Also shown in the figure are the theoretical flat-plate pressure-ratio curves calculated from the boundary-layer interaction theory of reference 11. The pressure ratio variation on the flat plate was large in comparison with the maximum boundary-layer induced pressure ratio predicted by flat-plate theory. This difference in pressure ratios was probably caused by the static-pressure variation in the jet test section. It should be noted, however, that the maximum pressure on the flat-plate model was only about 10 percent above free-stream static pressure. It should be further noted that the pressure increase due to the shock—boundary-layer interaction in the vicinity of the corner was clearly evident regardless of the pressure variations previously described.

In figure 5, the ratio  $(P_c - P_{fp})/P_{fp}$ , which represents the increase in static pressure on the corner model over that for the flat plate, is plotted against model length for several values of y and several unit Reynolds numbers. The results indicate that in the vicinity of the corner the static pressure on the corner model was as much as 10 to 12 percent greater than that on the flat plate for the same test conditions.

There are variations in the pressure along the length of the corner model for the two stations nearest the corner, and these variations are repeatable. It is not known whether these variations are due to corner or test-section effects. Variations similar to those shown in figure 5 have been reported by Bogdonoff and Vas (ref. 12) from preliminary tests conducted in the Helium Hypersonic Wind Tunnel of Princeton University. They tentatively attributed the pressure variations in the vicinity of the corner to a shock-induced vortex system generated at the leading edge of the corner.

Figure 5 shows that the distance from the leading edge at which the peak pressure rise occurred increased as the distance from the corner increased. This result is to be expected since any disturbance caused by the corner would originate at the leading edge of the corner and spread outward from the corner as the distance from the leading edge increased. As the distance from the corner increased, the peak and average values of the pressure rise due to the corner tended to decrease.

The percentage of increase in the pressure in the vicinity of the corner was almost constant with respect to the unit Reynolds number. There was, however, a slight indication that the increase in pressure due to the corner increased as the unit Reynolds number decreased; and this trend might be expected from boundary-layer interaction theory.

There were indications (fig. 5) that the pressure on the corner model was about 2 percent higher than that for the flat plate in regions where the corner effect would not be expected to be present ( $y = 1.50$ , e.g.). This discrepancy in pressure is noted, but no explanation for it is known.

## Heat-Transfer Data

The heat-transfer data for the corner model are presented in figure 6 in the form of Stanton number plotted against Reynolds number. The theoretical value for the flat-plate Stanton number for a laminar boundary layer for an insulated plate and for a turbulent boundary layer is also shown in figure 6. Theoretical values for the laminar- and turbulent-flow Stanton number were obtained from references 13 and 14, respectively. The temperature ratio  $T_w/T_\infty$  for the theoretical turbulent-boundary-layer curve was taken as 4.0 since this value closely approximated the ratio for this investigation.

Figure 6 indicates that the effect of the corner resulted in an increase in the heat-transfer rate in the vicinity of the corner for flow that, for the same Reynolds number, would be laminar on a flat plate. This increase could be as high as 50 percent greater than theoretical flat-plate laminar-boundary-layer heat-transfer rates for stations 0.10 inch from the corner. The effect of the corner on heat transfer in the laminar-flow region decreased as the distance from the corner increased; and at  $y = 1.50$  inches, the effect of the corner appeared to be absent for the length of the model. Figure 6 also indicates that the effect of the corner decreased as unit Reynolds number increased. There appeared to be a negligible influence of the corner on the turbulent-boundary-layer heat-transfer rate and on the transition Reynolds number. There was some evidence (fig. 6) that the high heat-transfer region in the vicinity of the corner was not uniform. This result might be expected as a result of the pressure variation along the model at the two stations nearest the corner.

The tendency of the corner to increase the laminar-flow heat-transfer rate in the vicinity of the corner was probably due, in part, to the increase in static pressure. However, the increase of about 50 percent for the heat-transfer rate at  $y = 0.10$  appeared to be greater than can be attributed to the approximate 10-percent increase in pressure.

A temperature-sensitive paint investigation was conducted to gain additional information on the heat-transfer rate in the vicinity of the corner. The paint used in this investigation had the characteristic that a pronounced color change occurred at a known temperature. However, the gray tone of the colors involved were almost identical when recorded on black and white film, and efforts to reproduce the photographs showing the color changes were not successful enough to warrant inclusion of these reproductions in the report. The results, observed visually, indicated high heat-transfer regions in the vicinity of the corner, and these regions appeared to originate at the leading edge of the corner. In general, the high heat-transfer region was confined to an area in the vicinity of the corner. The results of this investigation confirmed the results obtained with the heat-transfer model and served to supplement these results by visually indicating the extent

of the high heat-transfer region. The results also showed several other areas with higher heating rates than the general level, and these could be attributed to the leading-edge, transition, and end effects.

The visual results, plus the pressure and heat-transfer results, tend to confirm the tentative postulation of Bogdonoff and Vas (ref. 12), which attributed the pressure variation in the vicinity of the leading edge of a corner to a shock-induced vortex system that is generated by the leading edge of the corner.

L  
5  
2  
1 A light area in the immediate vicinity of the corner disclosed by the temperature sensitive paint investigation indicated a region of low heat-transfer rate. This region could probably be attributed to the interaction of the normally undisturbed flat-plate boundary layer in the vicinity of the corner as predicted from the incompressible-flow theory of references 2, 3, 4, and 5. This region did not appear to extend to the instrumented stations nearest the corner and, therefore, is not shown in figure 6, except possibly at a unit Reynolds number of  $1.95 \times 10^6$  for stations 0.10 inch from the corner.

#### CONCLUSIONS

An experimental investigation was made to determine the effects of the shock—boundary-layer interaction on the static pressure and heat-transfer rate in the vicinity of an interior corner formed by the normal intersection of two planes where the line of intersection was aligned with the free-stream velocity. The investigation was made at a nominal Mach number of 4.95 and a stagnation temperature of 400° F. The nominal Reynolds number for the heat-transfer investigation ranged from  $1.95 \times 10^6$  to  $74.17 \times 10^6$  per foot and for the pressure test, from  $15.19 \times 10^6$  to  $74.17 \times 10^6$  per foot.

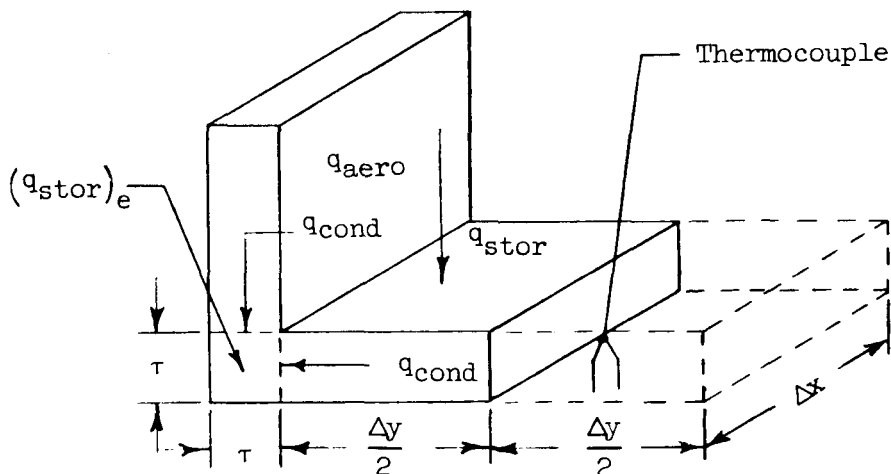
The results of the investigation indicated that the static pressure in the vicinity of the corner was from 10 to 12 percent greater than the pressure on a flat plate for the same free-stream conditions. The heat-transfer investigation indicated that the laminar-flow heat-transfer rate in the vicinity of the corner was higher than theoretical values for a flat plate at the same test conditions. For a unit Reynolds number of  $3.39 \times 10^6$  per foot, the increase was about 50 percent for stations 0.10 inch from the corner. The effect of the corner on the heat-transfer rate decreased with both distance from the corner and increasing unit Reynolds number. There was a negligible effect of the corner on the turbulent-flow heat-transfer rate and the transition Reynolds number.

Langley Research Center,  
National Aeronautics and Space Administration,  
Langley Field, Va., September 3, 1959.

## APPENDIX

APPROXIMATE METHODS FOR ESTIMATING ERROR CAUSED  
BY EXCESS MASS IN THE CORNER

An approximate analysis for the conduction effect of the 0.030- by 0.030-inch excess mass at the corner on the heat-transfer rate, computed from the data obtained with the thermocouple located 0.10 inch from the corner, can be made by considering the heat balance for an elementary volume shown in the figure below:



Since the effect of radiation can be neglected, the heat balance for the volume  $\tau \Delta x \Delta y$  is

$$q_{aero} = q_{stor} + q_{cond} \quad (A1)$$

If it is assumed that the temperature of the element is constant over its volume or that the temperature of the thermocouple located at  $\Delta y/2$  measures the mean temperature of the element, then the heat-storage rate, also noted as the apparent aerodynamic heating rate, is given by

$$q_{stor} = \Delta x \Delta y \tau \rho_m c_m \frac{\partial T_m}{\partial t} \quad (A2)$$

It has been previously demonstrated in the section entitled "Reduction of Data" that conduction effects are negligible except possibly in the vicinity of the corner; therefore, it is reasonable to assume that the heat conducted from the volume  $\tau \Delta x \Delta y$  is stored in the excess mass in the corner. The heat conduction rate from the elementary volume will be one-half of the heat-storage rate in the excess mass since heat is conducted to this mass through two faces. Thus, the heat conduction rate from  $\tau \Delta x \Delta y$  to the excess mass is

$$q_{\text{cond}} = \frac{1}{2} (q_{\text{stor}})_e \quad (\text{A3})$$

and the heat-storage rate for the excess mass is

$$(q_{\text{stor}})_e = \tau^2 \Delta x \rho_m c_m \left( \frac{\partial T_m}{\partial t} \right)_e \quad (\text{A4})$$

To find the ratio of the true aerodynamic heating rate to the apparent heating rate, the following ratio is formed:

$$\frac{q_{\text{aero}}}{(q_{\text{aero}})_a} = 1 + \frac{\tau \left( \frac{\partial T_m}{\partial t} \right)_e}{2 \Delta y \frac{\partial T_m}{\partial t}} \quad (\text{A5})$$

For the present investigation,  $\tau = 0.030$  inch and  $\frac{\Delta y}{2} = 0.10$  inch.

From equation (A5), it can be seen that if the change in temperature with respect to time for the excess mass approaches the value for the elementary volume, the maximum error possible is 7.5 percent.

## REFERENCES

1. Bertram, Mitchel H., and Henderson, Arthur, Jr.: Effects of Boundary-Layer Displacement and Leading-Edge Bluntness on Pressure Distribution, Skin Friction, and Heat Transfer of Bodies at Hypersonic Speeds. NACA TN 4301, 1958.
2. Loiziansky, L. G.: Interference of Boundary Layers. No. 249, Trans. Central Aero-Hydrodynamical Inst. (Moscow), 1936.
3. Loitsianskii, L. G., and Bolshakov, V. P.: On Motion of Fluid in Boundary Layer Near Line of Intersection of Two Planes. NACA TM 1308, 1951.
4. Carrier, G. F.: The Boundary Layer in a Corner. Quarterly of Appl. Math., vol. IV, no. 4, Jan. 1947, pp. 367-370.
5. Sowerby, L., and Cooke, J. C.: The Flow of Fluid Along Corners and Edges. Quarterly Jour. of Mech. and Appl. Math., vol. VI, pt. 1, Mar. 1953, pp. 50-70.
6. Cooper, Morton, and Mayo, Edward E.: Measurements of Local Heat Transfer and Pressure on Six 2-Inch-Diameter Blunt Bodies at a Mach Number of 4.95 and at Reynolds Numbers Per Foot Up to  $81 \times 10^6$ . NASA MEMO 1-3-59L, 1959.
7. Carslaw, H. S., and Jaeger, J. C.: Operational Methods in Applied Mathematics. Oxford University Press, 1941.
8. Carslaw, H. S., and Jaeger, J. C.: Conduction of Heat in Solids. The Clarendon Press (Oxford), 1947.
9. Anon.: The Physical Properties of a Series of Steels.—Part II. Alloy Steels Res. Comm. Paper No. 23/1946, The Iron and Steel Inst., Sept. 1946.
10. Hilsenrath, Joseph, Beckett, Charles W., et al.: Tables of Thermal Properties of Gases. NBS Cir. 564, U.S. Dept. Commerce, 1955.
11. Bertram, Mitchel H.: Boundary-Layer Displacement Effects in Air at Mach Numbers of 6.8 and 9.6. NACA TN 4133, 1958.
12. Bogdonoff, S. M., and Vas, I. E.: A Preliminary Investigation of the Flow in a  $90^\circ$  Corner at Hypersonic Speeds. Part I - Flat Plates With Thin Leading Edges at Zero Angle of Attack. D143-978-013(ARDC TR 57-202, AD 150 023), Bell Aircraft Corp., Dec. 20, 1957.

L  
5  
2  
1

13. Van Driest, E. R.: The Laminar Boundary Layer With Variable Fluid Properties. Rep. No. AL-1866, North American Aviation, Inc., Jan. 19, 1954.
14. Van Driest, E. R.: The Problem of Aerodynamic Heating. Aero. Eng. Rev., vol. 15, no. 10, Oct. 1956, pp. 26-41.

TABLE I.- PRESSURE-ORIFICE STATION LOCATION

y, in.	x, in.						
0.10	0.25	0.75	1.50	2.50	4.00	6.00	8.00
.30	.25	.75	1.50	2.50	4.00	6.00	8.00
.70	.25	.75	1.50	2.50	4.00	6.00	8.00
1.50	.25	.75	1.50	2.50	4.00	6.00	8.00

TABLE II.- THERMOCOUPLE STATION LOCATION

y, in.	x, in.						
0	0.50	1.00	1.75	2.75	4.25	6.25	8.25
.10	.50	1.00	1.75	2.75	4.25	6.25	8.25
.30	.50	1.00	1.75	2.75	4.25	6.25	8.25
.70	.50	1.00	1.75	2.75	4.25	6.25	8.25
1.50	.50	1.00	1.75	2.75	4.25	6.25	8.25

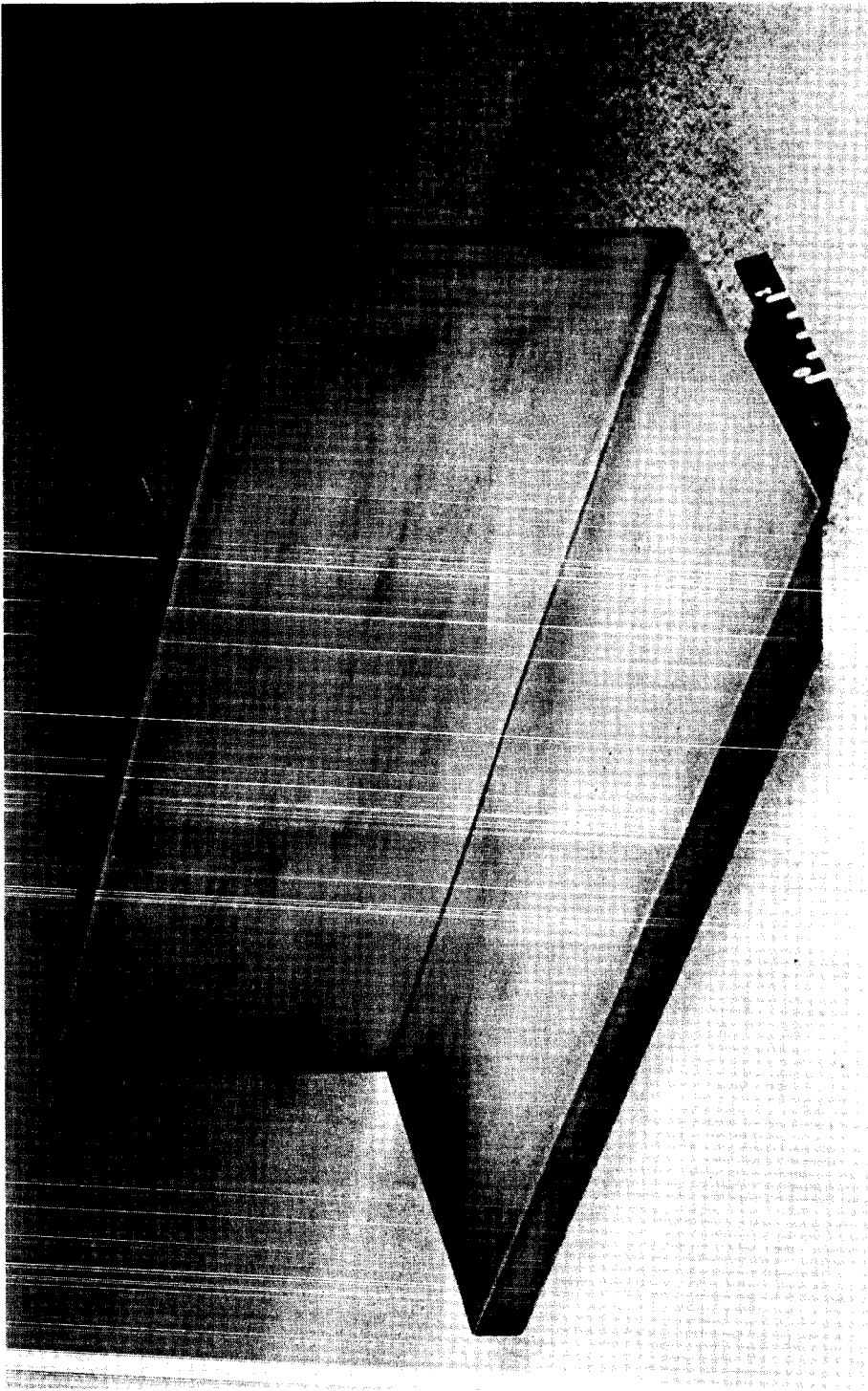


Figure 1.- Photograph of corner model. L-58-14

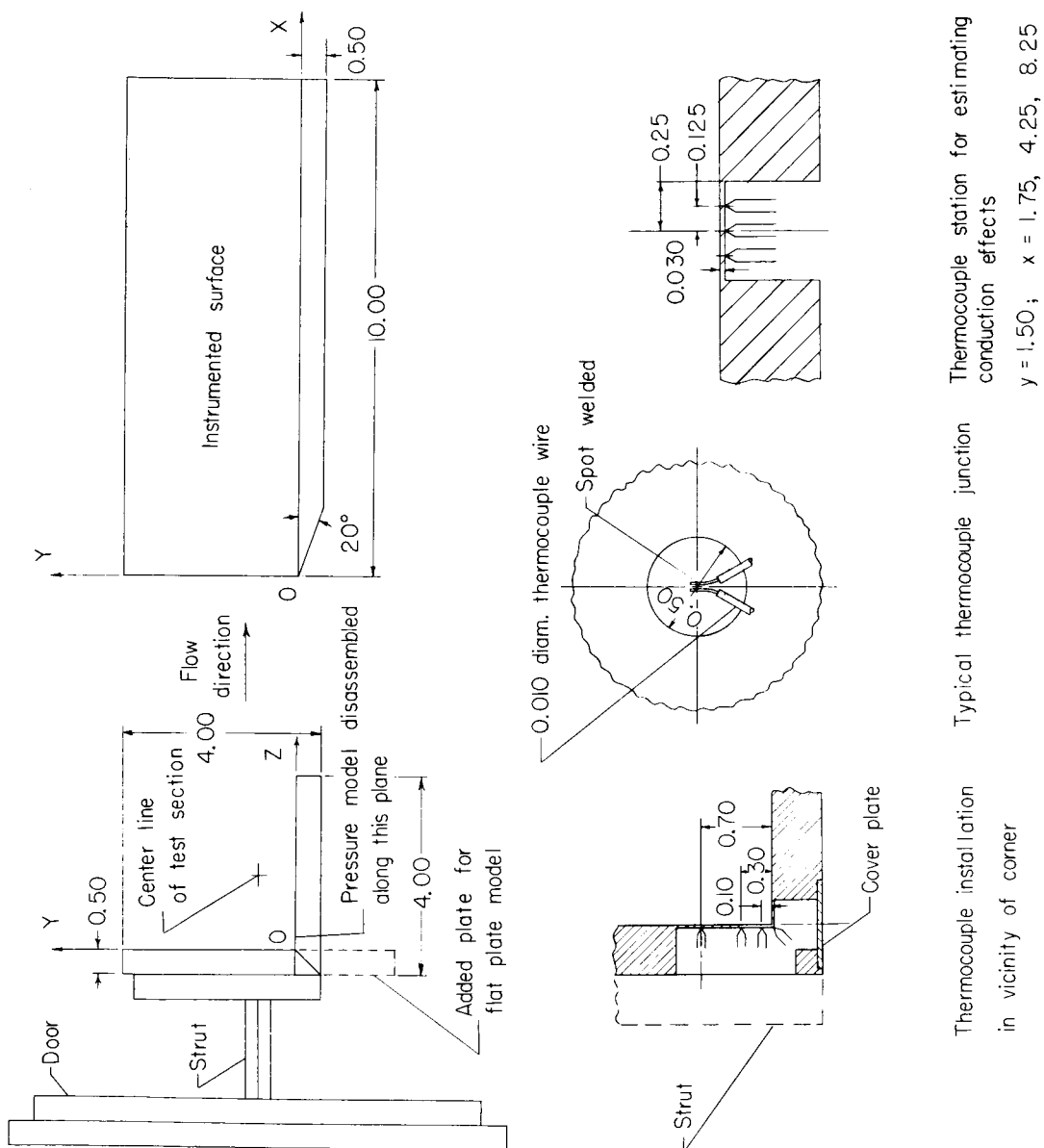
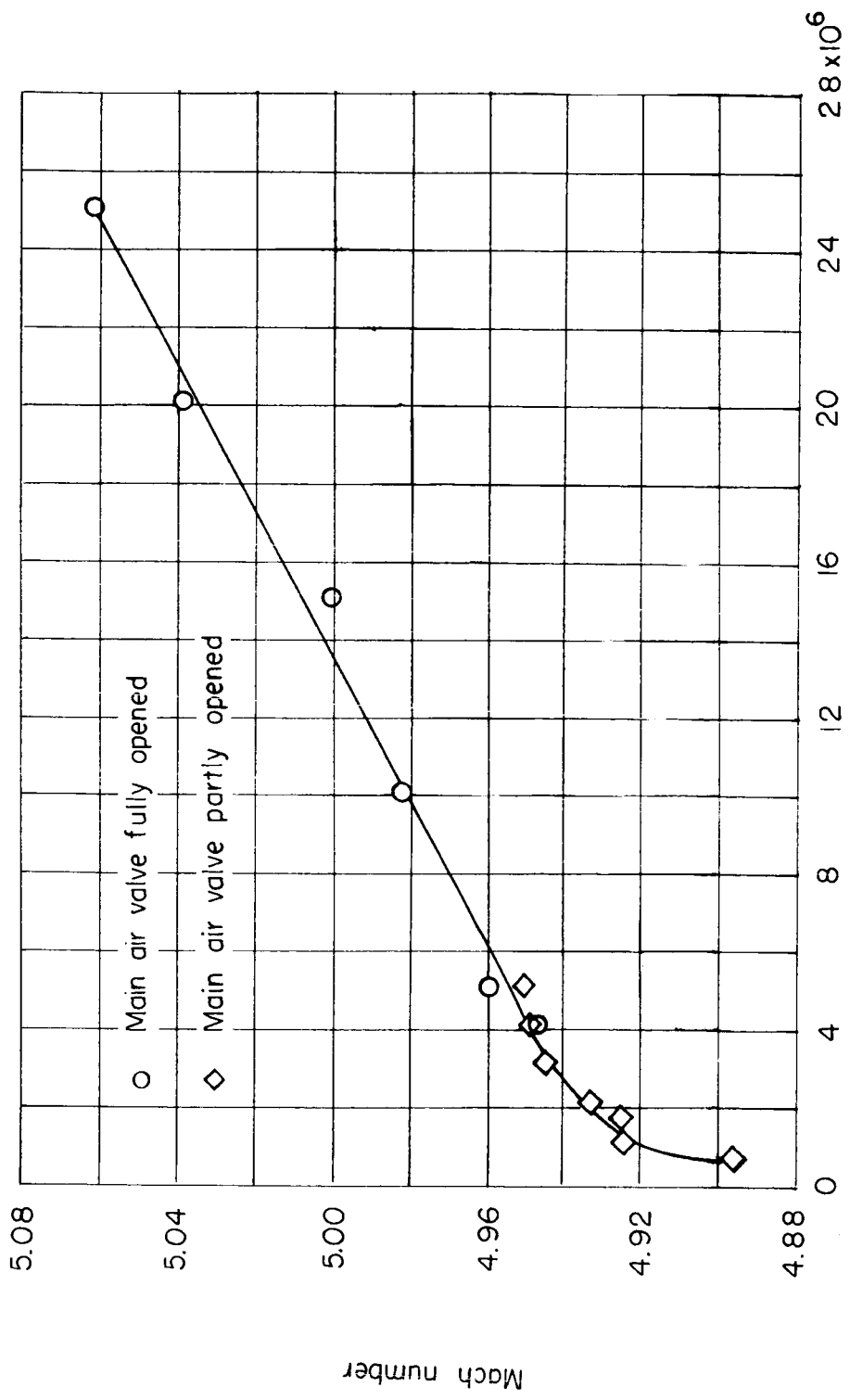


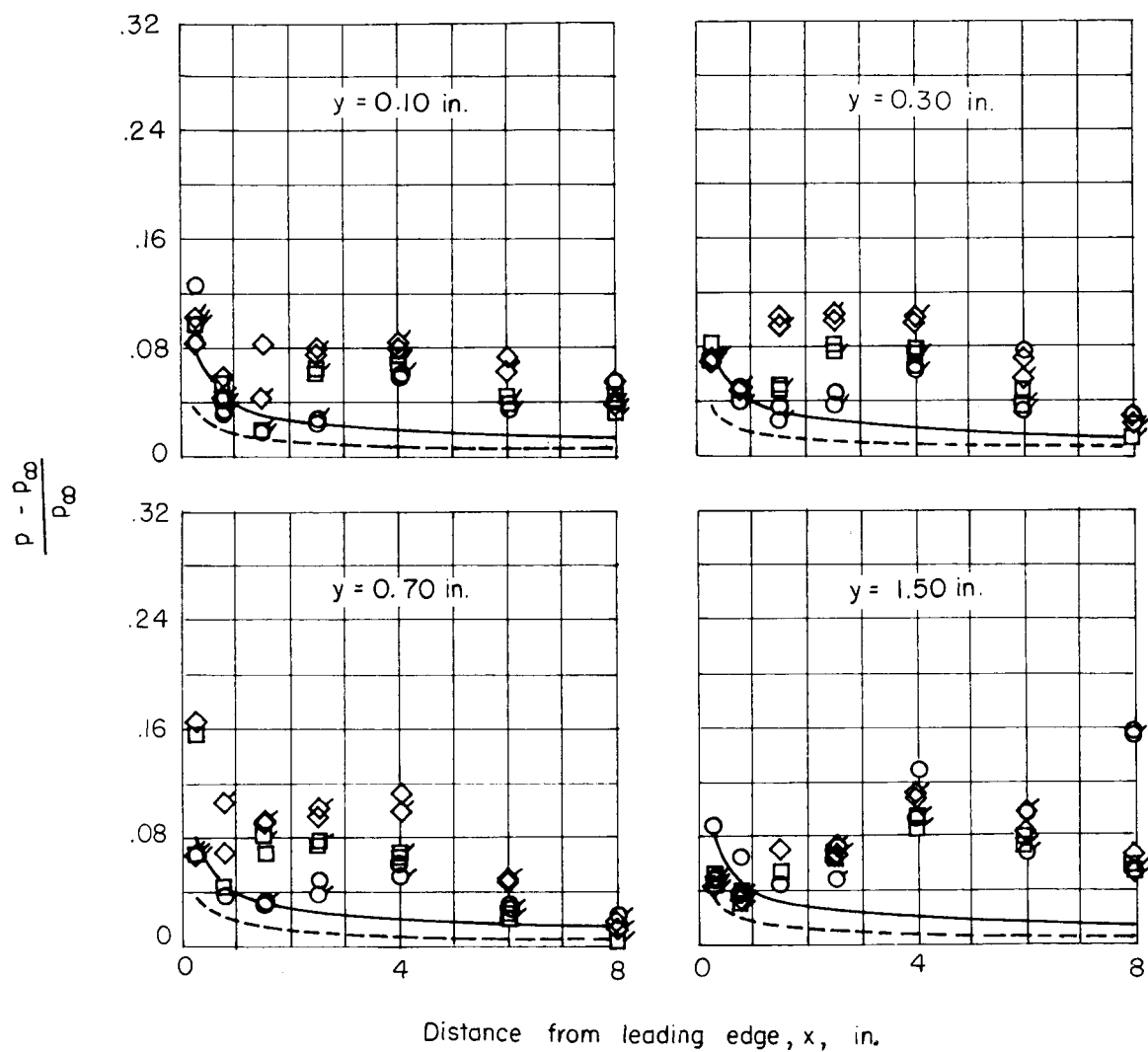
Figure 2.- General model dimensions. All dimensions are in inches except as noted.



Stagnation pressure,  $P_t$ ,  $\text{lb/sq in. abs}$

Figure 3.- Test-section Mach number variation with stagnation pressure.

Experiment	$N_{Re}$ , per foot
○	$15.19 \times 10^6$
□	44.68
◇	74.17
Theory, ref. 11	
—	15.19
- - -	74.17



(a) Flat-plate model.

Figure 4.- Static-pressure variation on model. Flagged symbols denote reruns.

Experiment     $N_{Re}$ , per foot

○            15.19 x 10

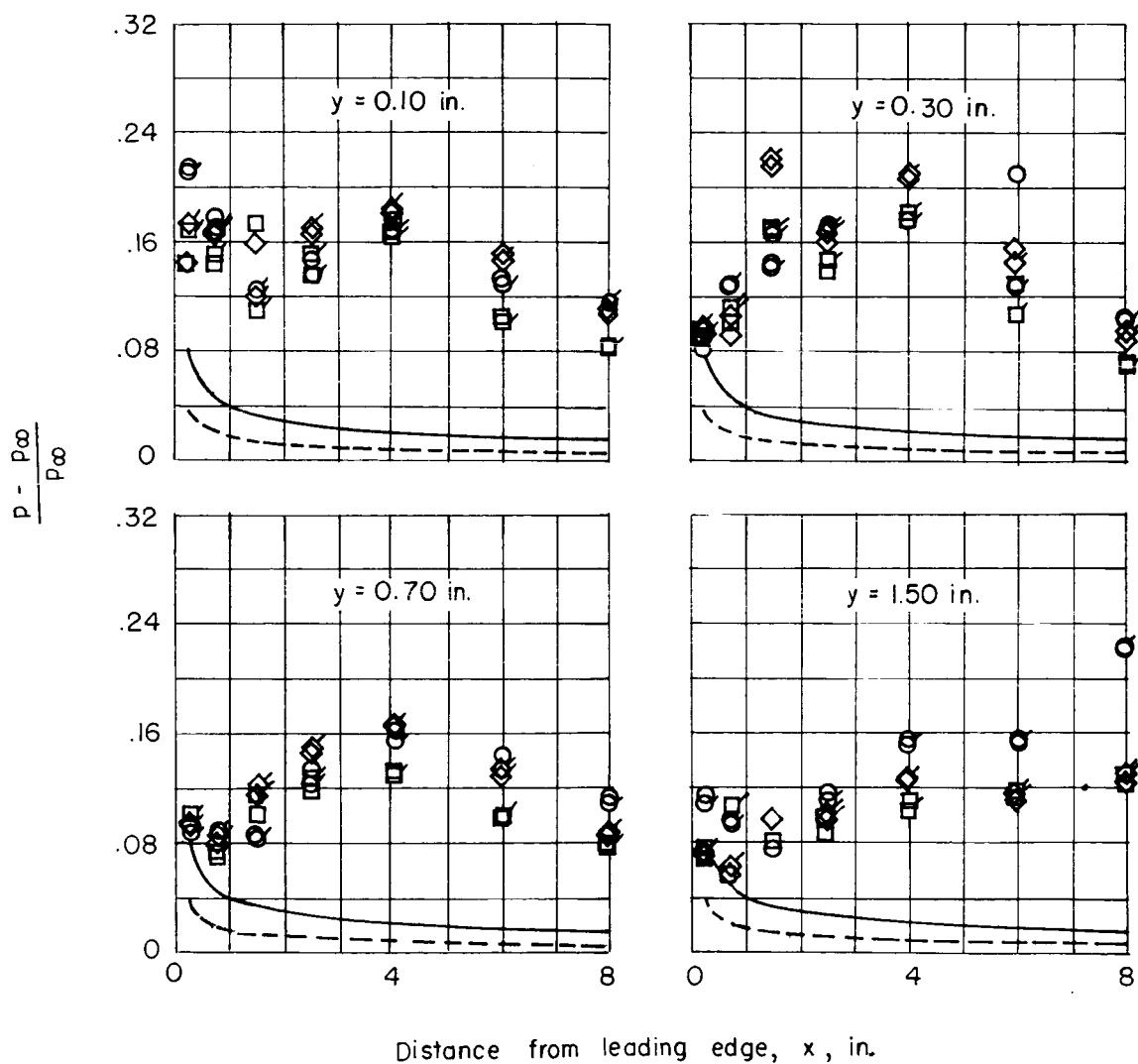
□            44.68

◇            74.17

Theory, ref. 11

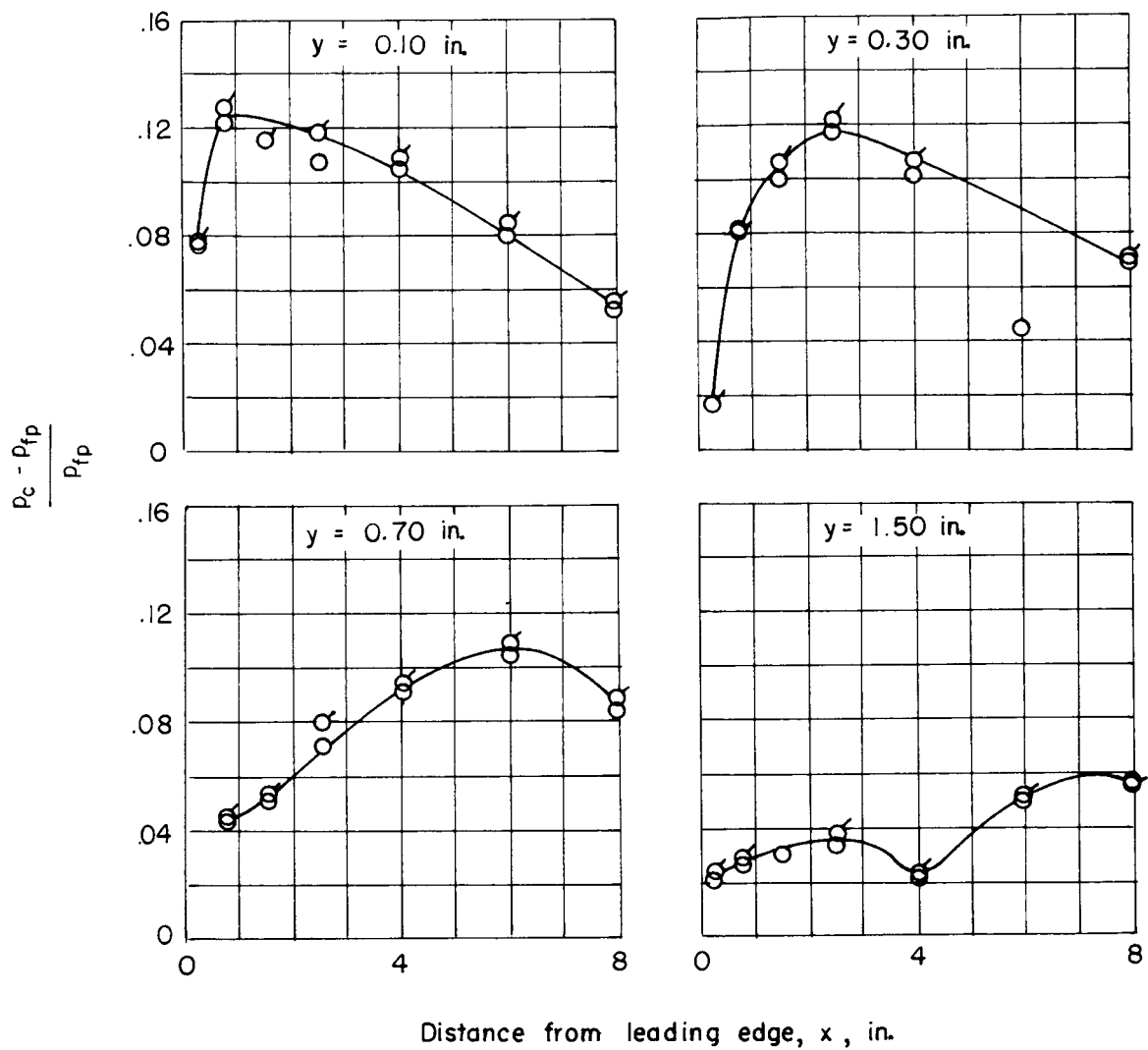
—            15.19

---          74.17



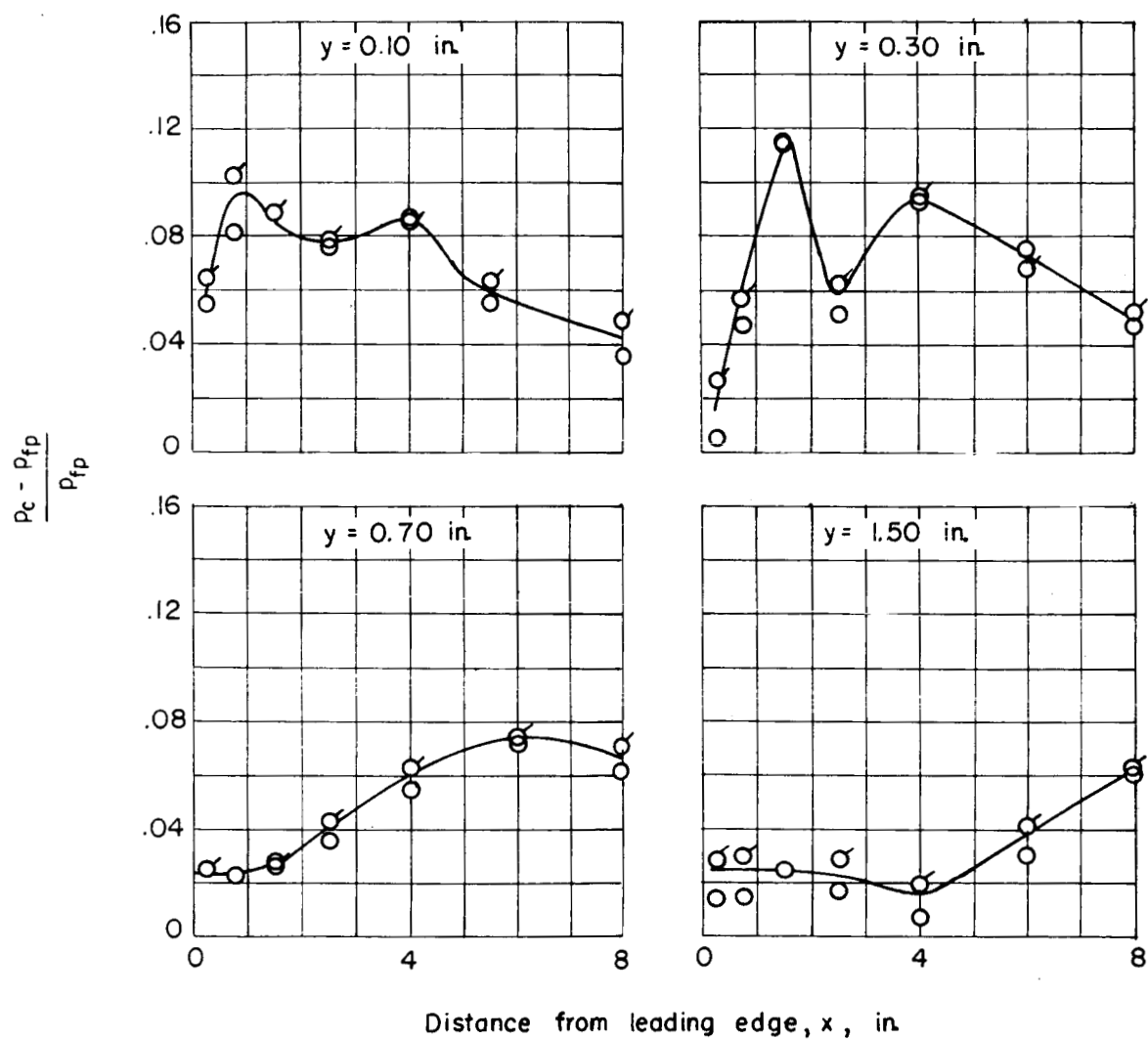
(b) Corner model.

Figure 4.- Concluded.



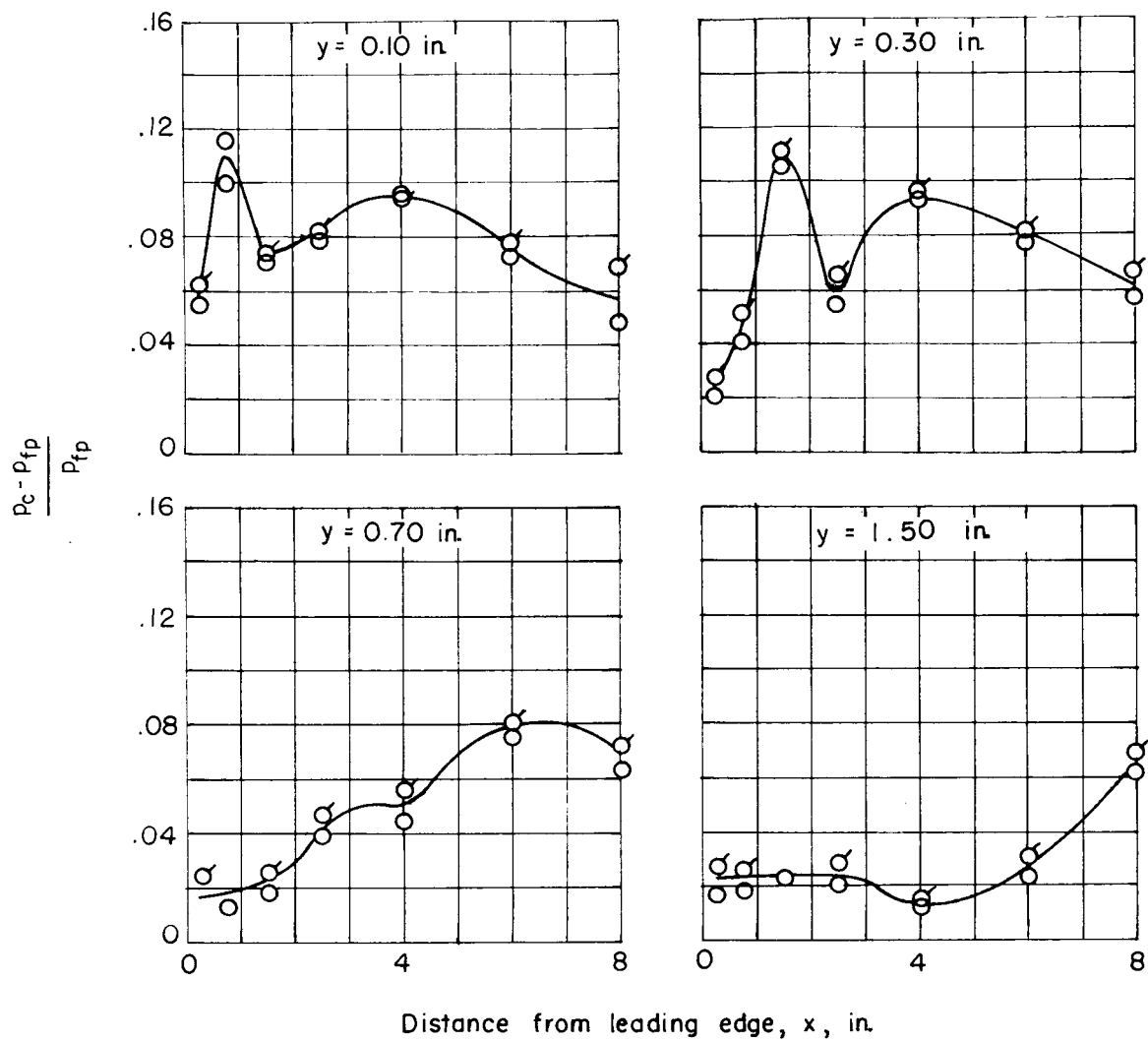
(a)  $N_{Re} = 15.19 \times 10^6$  per foot.

Figure 5.- Effect of corner on static pressure in vicinity of corner.  
Flagged symbols denote reruns.



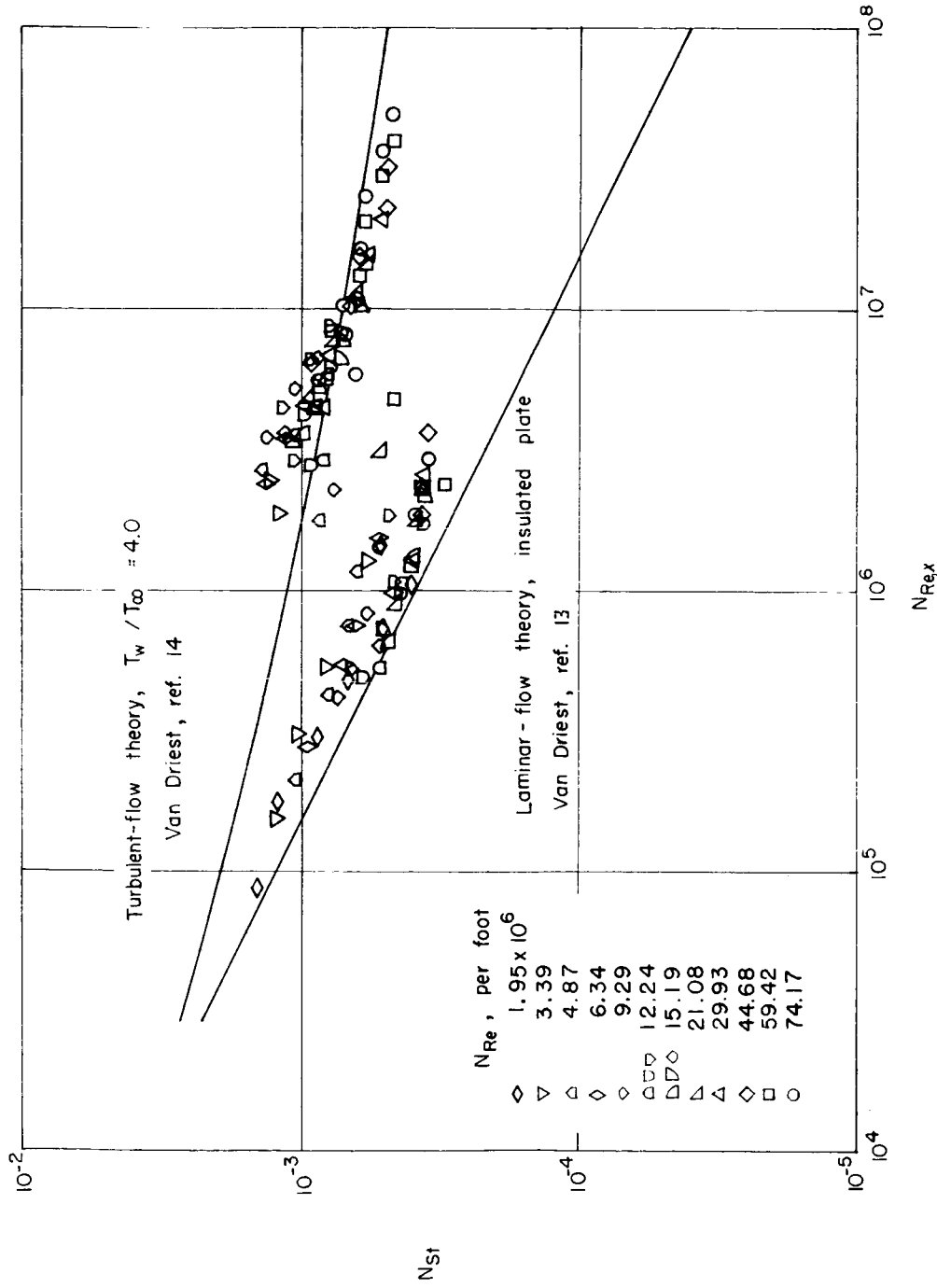
(b)  $N_{Re} = 44.68 \times 10^6$  per foot.

Figure 5.- Continued.



(c)  $N_{Re} = 74.17 \times 10^6$  per foot.

Figure 5.- Concluded.



(a)  $y = 0.10$  inch.

Figure 6.- Heat transfer to corner model.

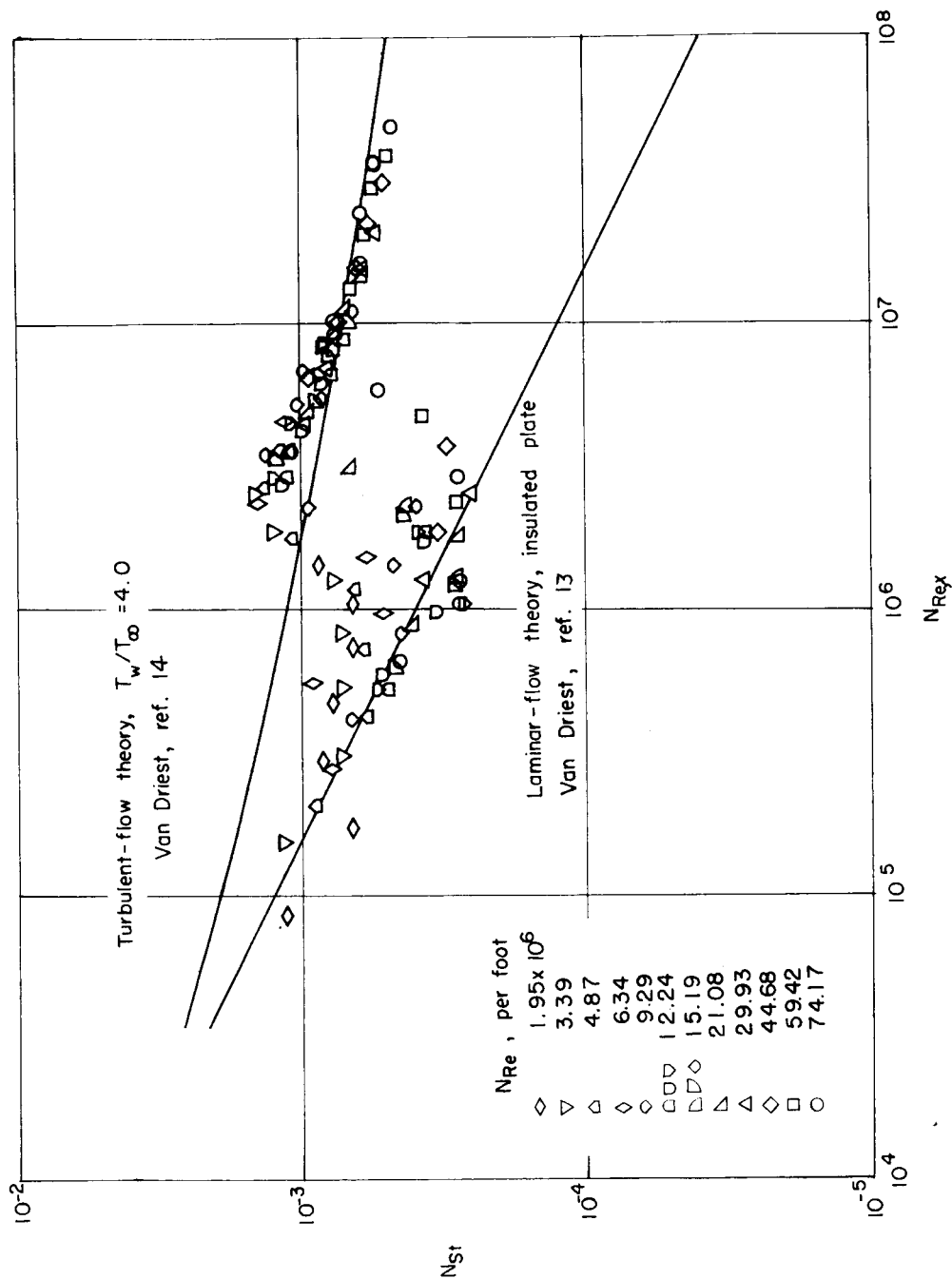
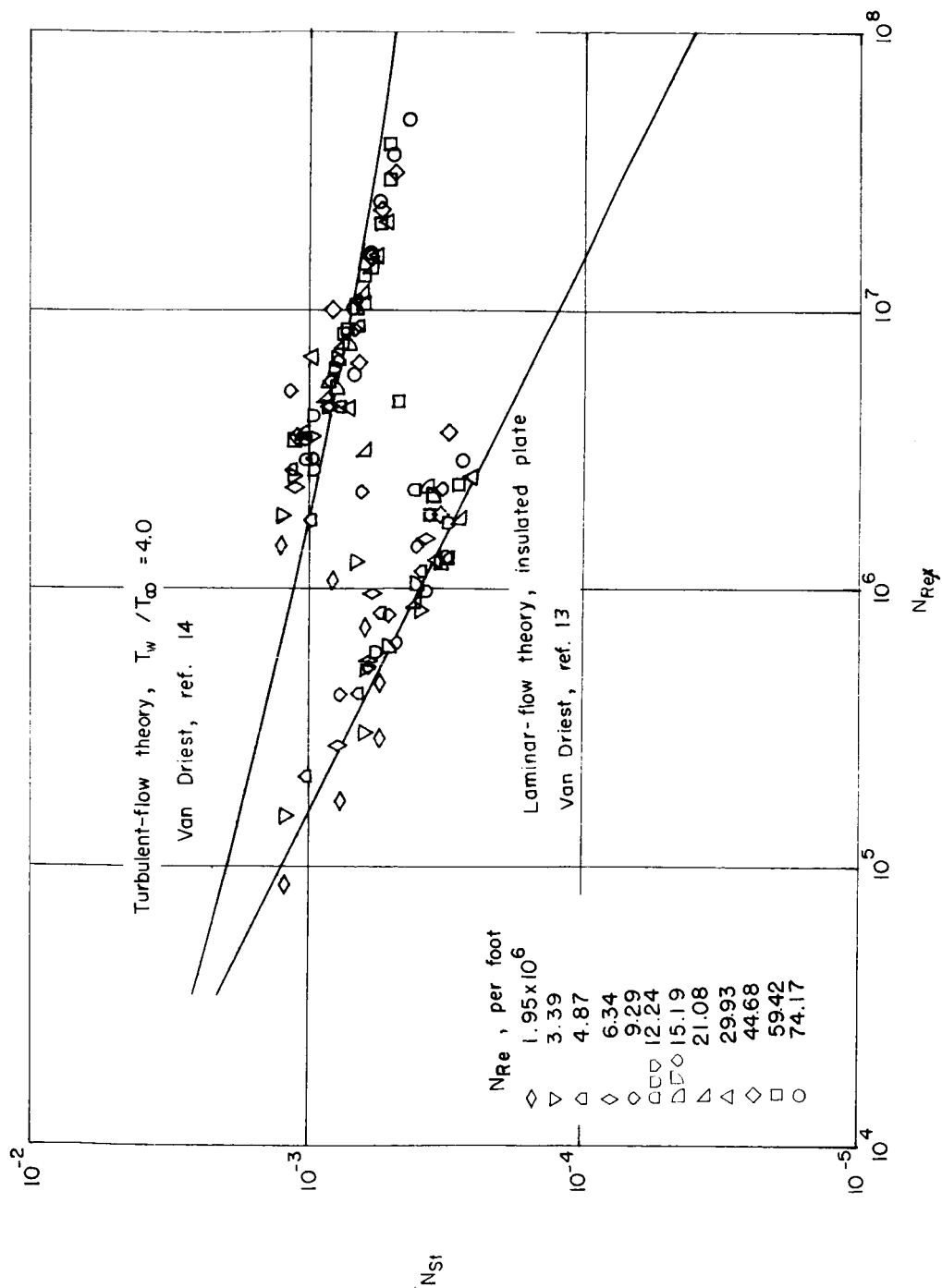
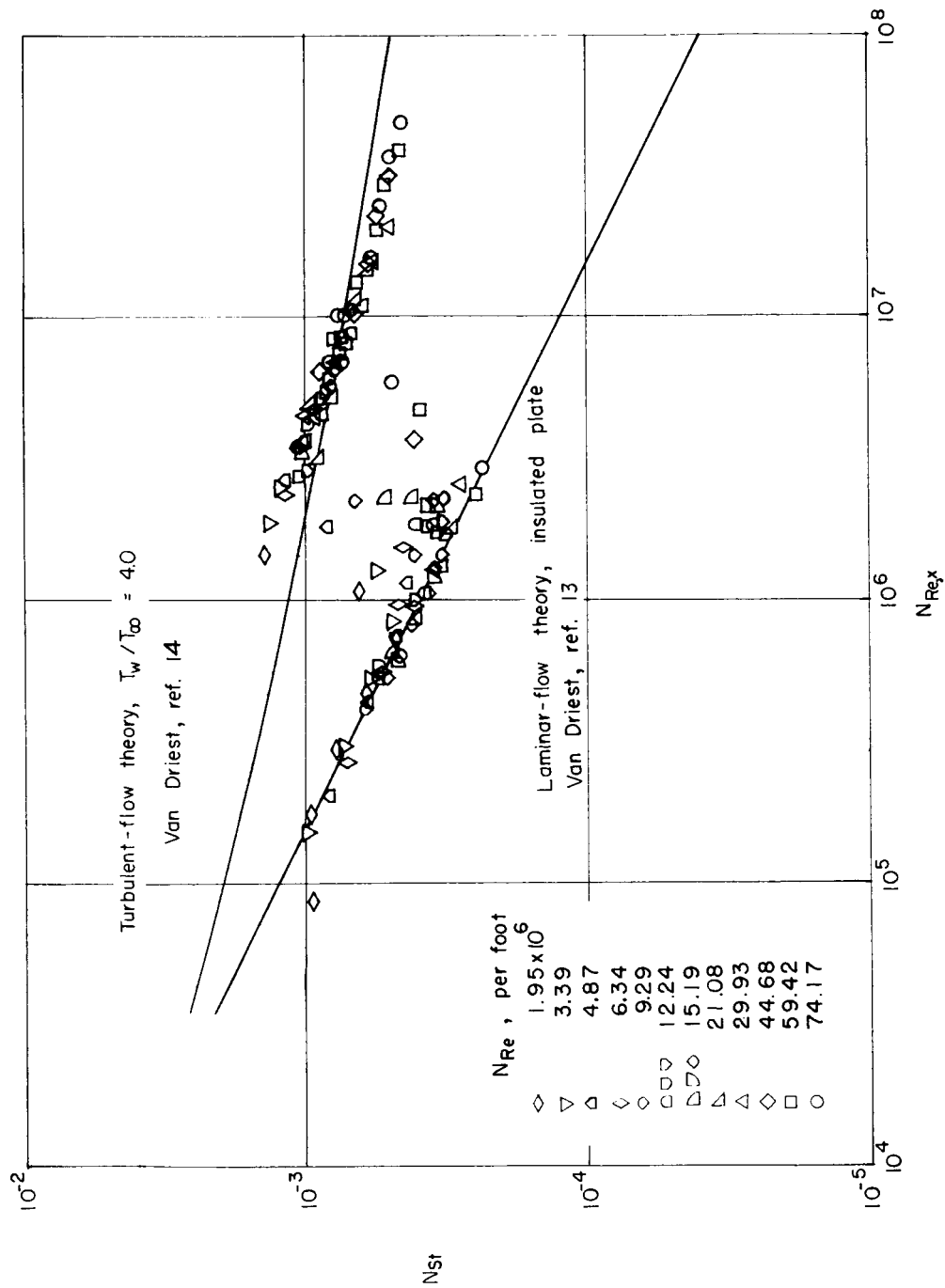
(b)  $y = 0.30$  inch.

Figure 6.- Continued.



(c)  $y = 0.70$  inch.

Figure 6.- Continued.



(d)  $y = 1.50$  inches.

Figure 6.- Concluded.